

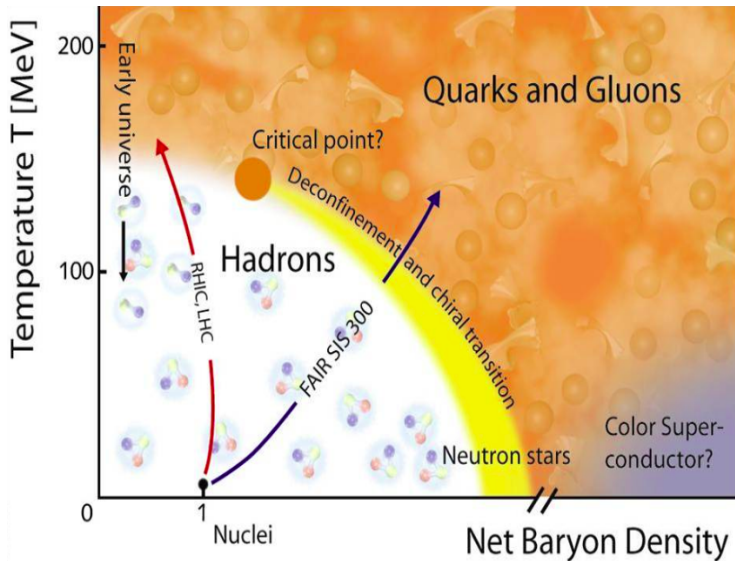
Confinement-deconfinement transition in dense SU(2) QCD

V. Braguta, V. Bornyakov, A. Kotov, I. Kudrov, A. Nikolaev

JINR, Dubna

10 July, 2017

QCD phase diagram



SU(3) QCD

- $Z = \int DUD\bar{\psi}D\psi \exp(-S_G - \int d^4x \bar{\psi}(\hat{D} + m)\psi) = \int DU \exp(-S_G) \times \det(\hat{D} + m)$
- Eigenvalues go in pairs $\hat{D} : \pm i\lambda \Rightarrow \det(\hat{D} + m) = \prod_{\lambda} (\lambda^2 + m^2) > 0$
i.e. one can use lattice simulation
- Introduce chemical potential: $\det(\hat{D} + m) \rightarrow \det(\hat{D} - \mu\gamma_4 + m) \Rightarrow$ the determinant becomes complex (**sign problem**)

SU(2) QCD

- $(\gamma_5 C \tau_2) \cdot D^* = D \cdot (\gamma_5 C \tau_2)$
- Eigenvalues go in pairs $\hat{D} - \mu\gamma_4 : \lambda, \lambda^*$
- For even N_f $\det(\hat{D} - \mu\gamma_4 + m) > 0 \Rightarrow$ **free from sign problem**

Differences between SU(3) and SU(2) QCD

- The Lagrangian of the SU(2) QCD has the symmetry: $SU(2N_f)$ as compared to $SU_R(N_f) \times SU_L(N_f)$ for SU(3) QCD
- Goldstone bosons ($N_f = 2$) $\pi^+, \pi^-, \pi^0, d, \bar{d}$

Similarities:

- There are transitions: confinement/deconfinement, chiral symmetry breaking/restoration
- A lot of observables are equal up to few dozens percent:

Topological susceptibility (Nucl.Phys.B715(2005)461):

$$\chi^{1/4}/\sqrt{\sigma} = 0.3928(40) (SU(2)), \quad \chi^{1/4}/\sqrt{\sigma} = 0.4001(35) (SU(3))$$

Critical temperature (Phys.Lett.B712(2012)279):

$$T_c/\sqrt{\sigma} = 0.7092(36) (SU(2)), \quad T_c/\sqrt{\sigma} = 0.6462(30) (SU(3))$$

Shear viscosity :

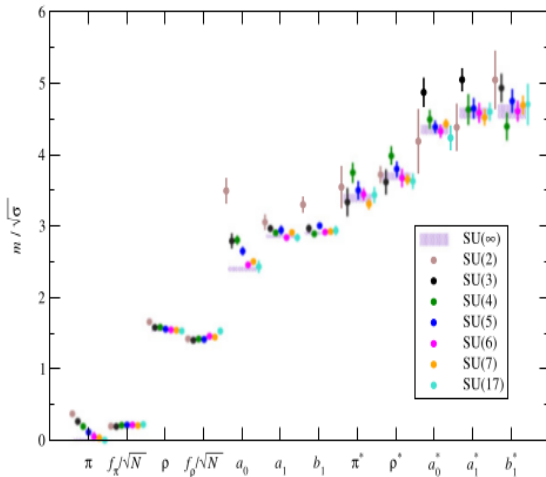
$$\eta/s = 0.134(57) (SU(2)), \quad \eta/s = 0.102(56) (SU(3))$$

JHEP 1509(2015)082

Phys.Rev. D76(2007)101701

Similarities:

- Spectroscopy (Phys.Rep.529(2013)93)



Similarities:

- Thermodynamic properties
- Some properties of dense medium (Phys.Rev.D59(1999)094019):

$$\Delta \sim \mu g^{-5} \exp\left(-\frac{3\pi^2}{\sqrt{2}g}\right)$$

To summarize:

- Dense SU(2) QCD can be used to study dense SU(3) QCD
 - Calculation of different observables
 - Study of different physical phenomena
- Lattice study of SU(2) QCD contains full dynamics of real system (contrary to phenomenological models)

To summarize:

- Dense SU(2) QCD can be used to study dense SU(3) QCD
 - Calculation of different observables
 - Study of different physical phenomena
- Lattice study of SU(2) QCD contains full dynamics of real system (contrary to phenomenological models)

The aim: numerical study of dense SU(2) QCD within lattice simulation

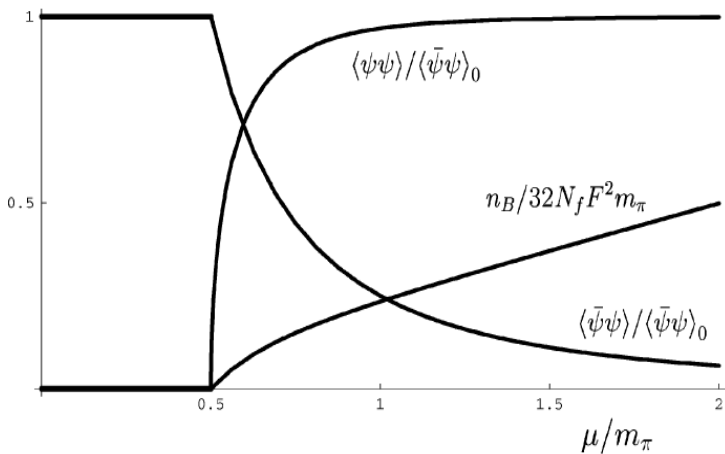
To summarize:

- Dense SU(2) QCD can be used to study dense SU(3) QCD
 - Calculation of different observables
 - Study of different physical phenomena
- Lattice study of SU(2) QCD contains full dynamics of real system (contrary to phenomenological models)

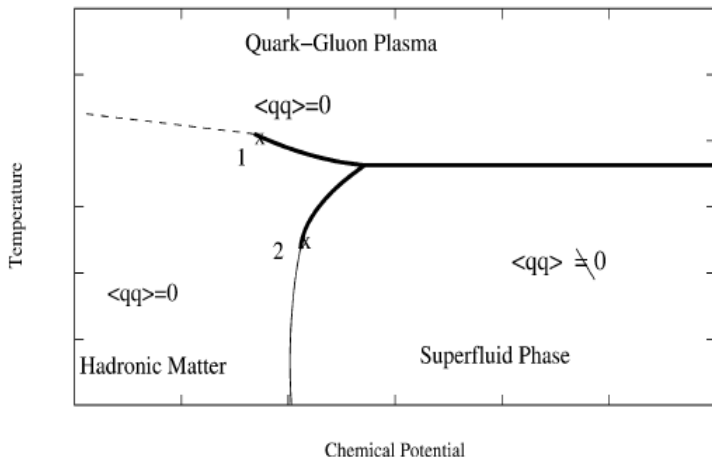
The aim: numerical study of dense SU(2) QCD within lattice simulation

- Study of gluon propagator, R. Rogalev
- See also talk of L. von Smekal

Predictions of CHPT



Staggered fermions $N_f = 4$



J.B. Kogut, D. Toublan, D.K. Sinclair, Nucl. Phys. B 642 (2002) 181–209

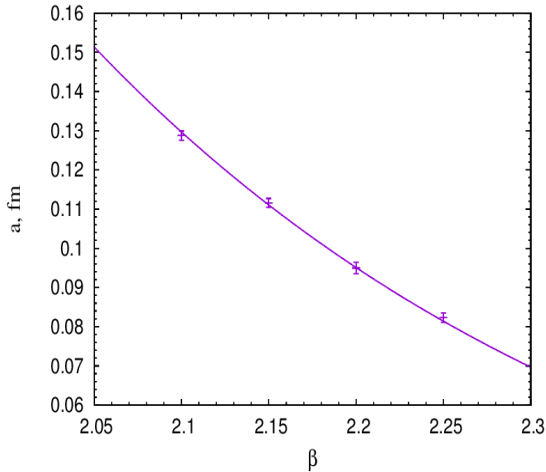
Details of the simulation (previous study):

- Staggered fermions with rooting: $N_f = 2$
- Lattice $16^3 \times 32$, $a = 0.11$ fm, $m_\pi = 362(4)$ MeV, $T = 55$ MeV
- Diquark source in the action $\delta S \sim \lambda \psi^T (C \gamma_5) \times \sigma_2 \times \tau_2 \psi$

- The symmetry breaking is different
 - Continuum: $SU(2N_f) \rightarrow Sp(2N_f)$
 - Staggered fermions: $SU(2N_f) \rightarrow O(2N_f)$
- Correct symmetry is restored in continuum limit
 - Naive limit $a \rightarrow 0$: two copies of $N_f = 2$ fundamental fermions
 - Correct spectroscopy (L. von Smekal)
 - Correct β function for $a < 0.17$ fm

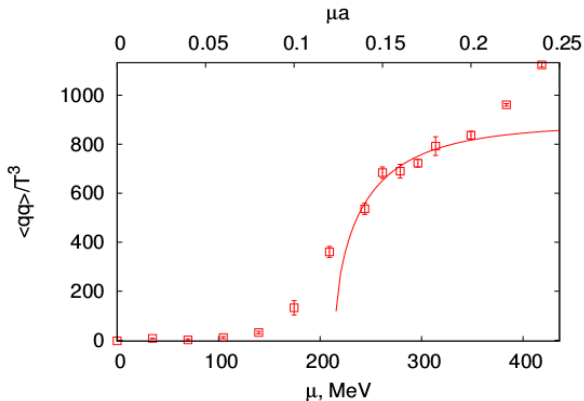
Beta function ($\beta = \frac{4}{g^2}$)

Two loops, $N_f = 2$ fundamental fermions



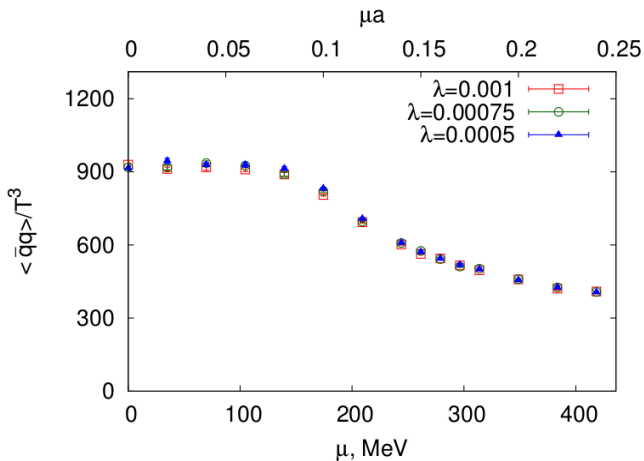
Small chemical potential
 $\mu < 350 \text{ MeV}$

Diquark condensate



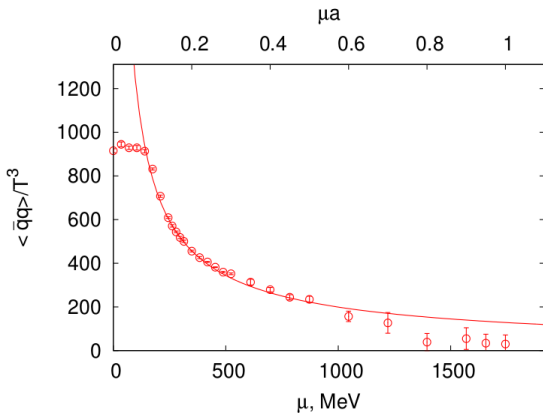
- Good agreement with CHPT $\langle \psi \psi \rangle / \langle \bar{\psi} \psi \rangle_0 = \sqrt{1 - \frac{m_\pi^4}{\mu^4}}$
- Phase transition at $\mu \sim m_\pi/2$
- Bose Einstein condensate (BEC) phase $\mu \in (200, 350)$ MeV

Chiral condensate



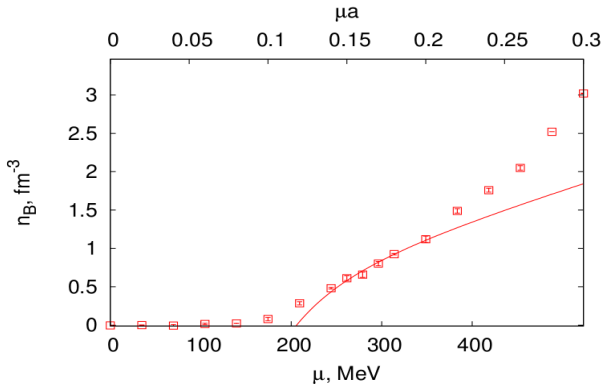
Good agreement with CHPT

Chiral condensate



- CHPT prediction $\langle \bar{\psi}\psi \rangle \sim \frac{m_\pi^2}{\mu^2}$
- We observe $\langle \bar{\psi}\psi \rangle \sim \frac{1}{\mu^\alpha}$, $\alpha \sim 0.6 - 1.0$

Baryon density



- Good agreement with CHPT $n \sim \mu - \frac{m_\pi^4}{\mu^3}$
- Phase transition at $\mu \sim m_\pi/2$
- Departure from CHPT predictions starts from $n \sim 1 \text{ fm}^{-3}$
- Transition: dilute baryon gas \rightarrow dense matter
- Baryon size in SU(2) \sim baryon size in SU(3) (agrees with QCD at large N_c)
- Large N_c starts already from $N_c = 2$?

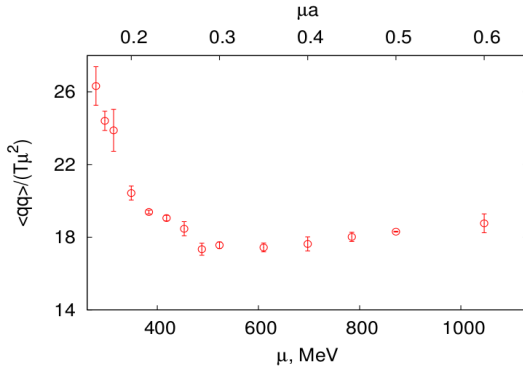
Large chemical potential
 $\mu > 350 \text{ MeV}$

Phase diagram for $N_c \rightarrow \infty$

(L. McLerran, R.D. Pisarski, Nucl.Phys. A796 (2007) 83-100)

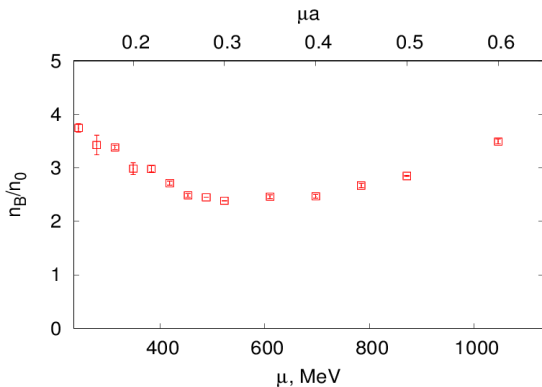
- Hadron phase $\mu < M_N/N_c$ ($p \sim O(1)$)
- Dilute baryon gas $\mu > M_N/N_c$ (width $\delta\mu \sim \frac{\Lambda_{QCD}}{N_c^2}$)
- Quarkyonic phase $\mu > \Lambda_{QCD}$ ($p \sim N_c$)
 - Degrees of freedom:
 - Baryons (on the surface)
 - Quarks (inside the Fermi sphere $|p| < \mu$)
 - No chiral symmetry breaking
 - The system is in confinement phase
- Deconfinement ($p \sim N_c^2$)

Diquark condensate



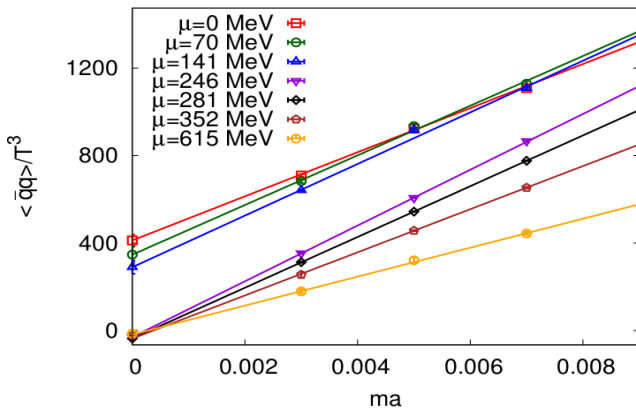
- Bardeen–Cooper–Schrieffer (BCS) phase $\mu > 500$ MeV, $\langle \psi \psi \rangle \sim \mu^2$
- **Baryons (on the surface)**

Baryon density



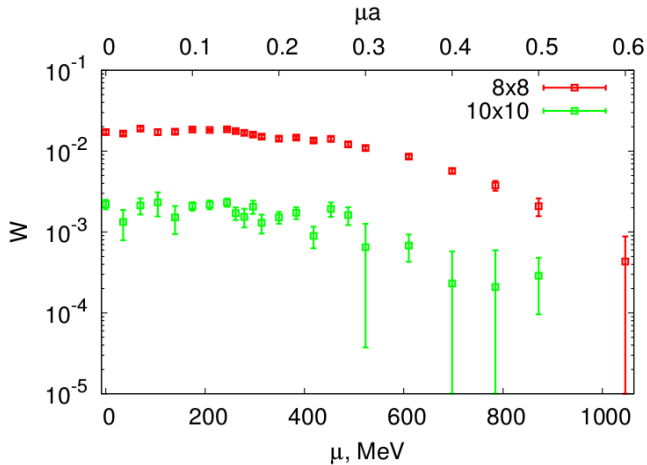
- Free quarks $n_0 = N_f \times N_c \times (2s + 1) \times \int \frac{d^3 p}{(2\pi)^3} \theta(|p| - \mu) = \frac{4}{3\pi^2} \mu^3$
- **Quarks inside Fermi sphere**
- Quarks inside Fermi sphere dominate over the surface:
 $\frac{4}{3}\pi\mu^3 > 4\pi\mu^2\Lambda_{QCD} \Rightarrow \mu > 3\Lambda_{QCD}$ ($n \sim (5 - 10) \times$ nuclear density)

Chiral condensate (chiral limit $m \rightarrow 0$)



No chiral symmetry breaking

Wilson loop



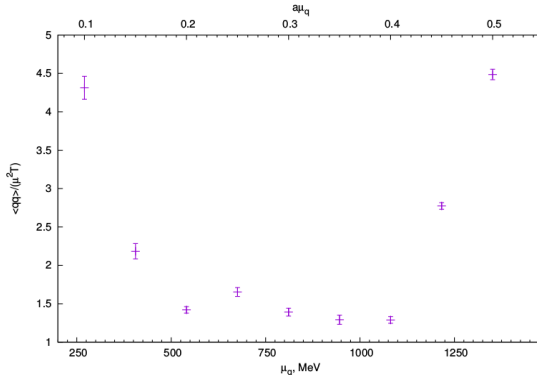
Polyakov loop is zero within the uncertainty of the calculation

Details of the simulation (present study):

- Tree-level improved gauge action
- $a = 0.073$ fm ($\sqrt{\sigma} = 440$ MeV)
present study: $\sqrt{\sigma}a = 0.16$ previous study: $\sqrt{\sigma}a = 0.29$
 \Rightarrow **closer to continuum limit**
- $m_\pi = 434(24)$ MeV ($m_\pi L_s \simeq 5$) new study: $m_\pi L_s \simeq 5$
previous study: $m_\pi L_s \simeq 3$
 \Rightarrow **Smaller final volume effects**
- Lattices
 - $32^3 \times 32$ ($T \simeq 0$)
 - $32^3 \times 24$ ($T \simeq 115$ MeV)
 - $32^3 \times 16$ ($T \simeq 180$ MeV)
 - $32^3 \times 8$ ($T \simeq 350$ MeV)
- Fixed λ parameter

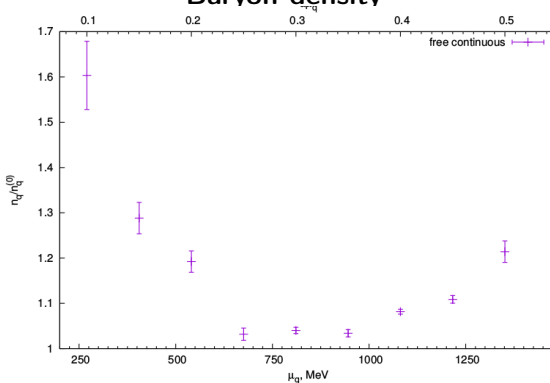
Preliminary results!

Diquark condensate



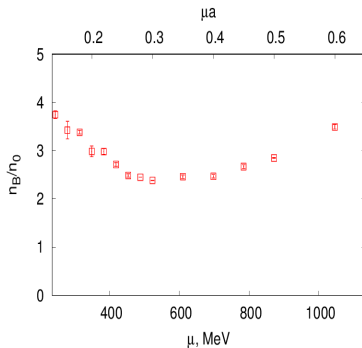
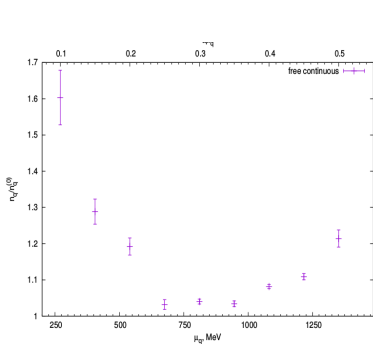
- Bardeen–Cooper–Schrieffer (BCS) phase $\mu > 500$ MeV ($\mu \sim 3\Lambda$), $\langle \psi\psi \rangle \sim \mu^2$ in agreement with our previous study
- **Baryons (on the surface)**

Baryon density



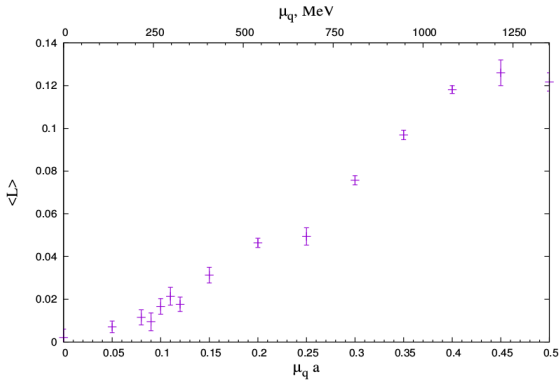
- Free quarks $n_0 = N_f \times N_c \times (2s + 1) \times \int \frac{d^3 p}{(2\pi)^3} \theta(|p| - \mu) = \frac{4}{3\pi^2} \mu^3$
- Smaller finite volume effects
- **Quarks inside Fermi sphere** $\mu > 500$ MeV
in agreement with our previous study
- We see BCS phase for different volumes and a (**Physical phase!**)

Baryon density



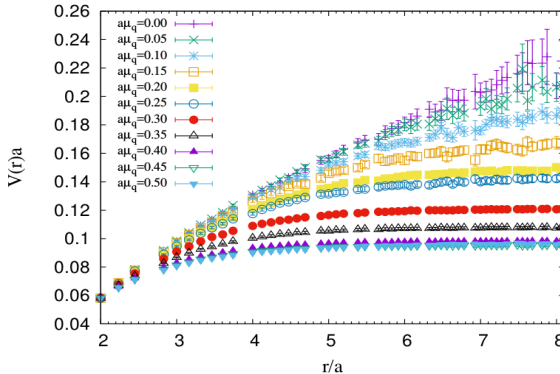
Finite volume effects are under control!

Polyakov loop



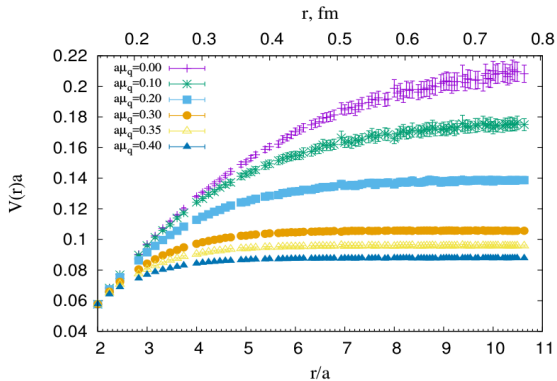
HYP + APE smearing were employed

Potential of static charges ($T \simeq 0$)

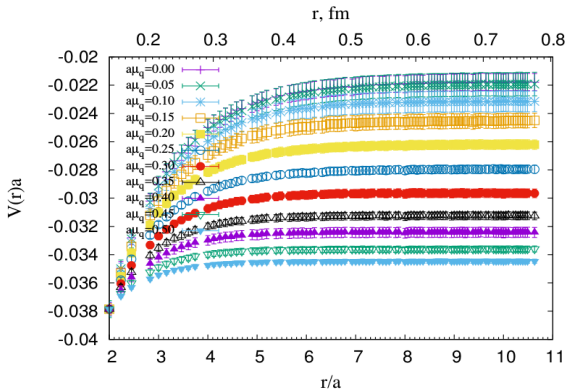


- Potentials were extracted from $\langle P(0)P^+(r) \rangle$
- HYP + APE smearing were employed
- We observe **deconfinement in dense medium!**

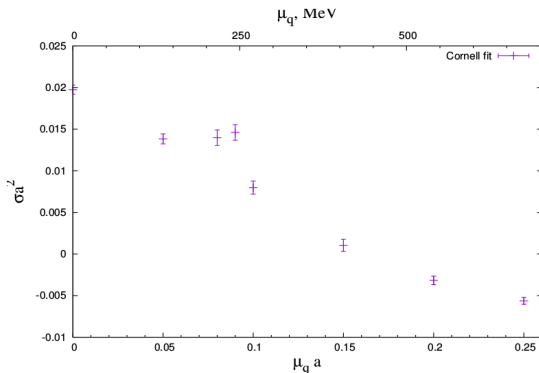
Potential of static charges ($T \simeq 115$ MeV)



Potential of static charges ($T \simeq 350$ MeV)



String tension



- Cornell potential $V(r) = A + \frac{B}{r} + \sigma r$
- Strongly depends on the interval
- For the region $r \in (3, 7)$ $\sigma < 0$ for the $a\mu \geq 0.2$

Debye screening

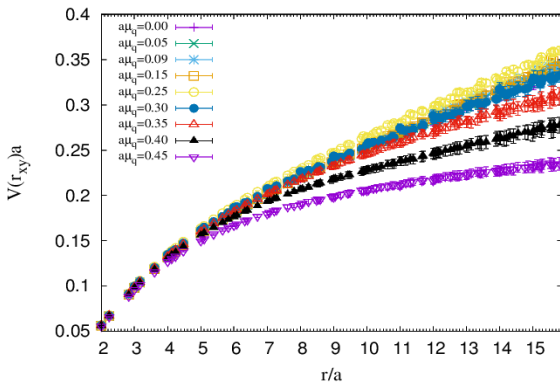
$a\mu_q$	μ_q , MeV	B	m_{Dq}	χ^2/dof
0.00	0.00	0.5307(89)	-0.1091(48)	10.689
0.05	135.14	0.4532(72)	-0.0380(46)	5.178
0.08	216.22	0.458(10)	0.0324(65)	3.889
0.09	243.25	0.4712(97)	0.0127(61)	3.316
0.10	270.27	0.4249(76)	0.0628(51)	2.753
0.15	405.41	0.474(13)	0.2355(81)	1.218
0.20	540.55	0.542(21)	0.390(12)	2.666
0.25	675.68	0.4662(89)	0.3645(56)	0.246
0.30	810.82	0.638(18)	0.6411(88)	0.316
0.35	945.96	0.641(21)	0.764(10)	0.135
0.40	1081.1	0.590(19)	0.8479(98)	0.153
0.45	1216.23	0.404(15)	0.742(11)	0.033
0.50	1351.37	0.2851(92)	0.5847(94)	0.047

- Debye potential $V(r) = A + \frac{B}{r} e^{-m_D r}$
- The fit is good for $a\mu \geq 0.25$

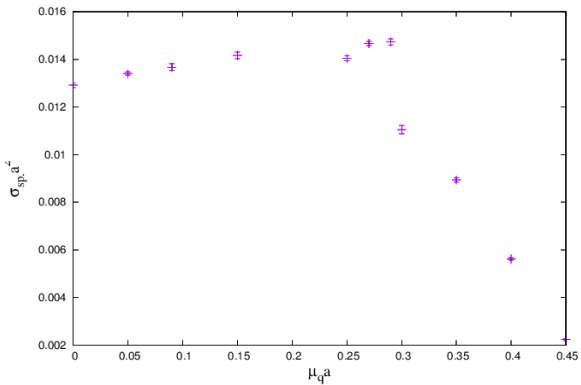
Spatial string tension:

- We measure Wilson loops in spatial directions
- Consider z direction as "time" and extract $V(r)$
- Fit our data for the $V(r)$ by the Cornell potential
- Determine spatial string tension

Spatial potential $V(r)$



Spatial string tension



Conclusion:

- We observe $\mu < m_\pi/2$ hadronic phase
- Transition to superfluid phase $\mu \simeq m_\pi/2$ (BEC)
- $\mu > m_\pi/2, \mu < m_\pi/2 + 150$ MeV dilute baryon gas
- Hadronic phase and BEC phase are well described by CHPT
- Deviation from CHPT from $\mu > 350$ MeV (dense matter)
- BCS phase $\mu \sim 500$ MeV, transition BEC \rightarrow BCS is smooth
- We observe deconfinement
- Difficult to determine critical chemical potential
($\mu \in (550, 800)$ MeV ?)

First observation of deconfinement in dense medium!

Second part: Confinement/deconfinement transition in dense matter and Abelian monopoles